Ephemeral microbial responses to pulses of bioavailable carbon in oxic and anoxic salt 1 marsh soils 2 3 Amanda C. Spivak^a, Andrew J Pinsonneault^a, Christopher Hintz^b, Jay Brandes^{a,c}, J Patrick 4 Megonigal^d 5 6 ^aUniversity of Georgia, Department of Marine Sciences, Athens, Georgia, USA 7 8 ^bSavannah State University, Department of Marine & Environmental Science, Savannah, 9 Georgia, USA ^cSkidaway Institute of Oceanography Savannah, Georgia, USA 10 ^dSmithsonian Environmental Research Center, Edgewater, Maryland, USA 11 12 Corresponding author: aspivak@uga.edu orcid.org/0000-0001-6743-0783 13 Andrew.Pinsonneault@uga.edu orcid.org/0000-0002-2665-1544 14 hintzc@savannahstate.edu https://orcid.org/0000-0003-4071-0165 15 Jay.Brandes@skio.uga.edu orcid.org/0000-0001-9911-4734 16 megonigalp@si.edu orcid.org/0000-0002-2018-7883 17 18 Running head: Rhizosphere responses to oxygen and C inputs 19 20 Keywords: Salt marsh, rhizosphere, organic carbon, redox, priming, sulfur oxidation 21

Abstract

22

23

24

25

26

27

28

29

30

31

32

33

34

35

36

37

38

39

40

41

42

43

Roots of salt marsh grasses contribute to soil building but also affect decomposition by releasing bioavailable carbon exudates and oxygen. Disentangling exudate and oxygen effects on decomposition is difficult in the field but essential for marsh carbon models and predicting the impacts of global change disturbances. We tested how pulsed, simulated exudates affect soil metabolism under oxic and anoxic conditions, and whether carbon and oxygen availability facilitate mineralization of existing organic matter (i.e., priming). We conducted a laboratory experiment in flow-through reactors, adding carbon pulses weekly for 84 days and then following starvation under low carbon conditions. Oxygen consumption and sulfide production were inhibited under anoxic and oxic conditions and slowed by 21±10% and 55±8%, respectively, between 1- and 5- days following exudate pulses. Respiration rates immediately following and between pulses increased over time, suggesting that microbes capitalize on and may acclimate to patchy resources. Starvation caused oxygen consumption and sulfide production to fall 28% and 78% in oxic and anoxic treatments. Smaller decreases in oxygen consumption following pulses could suggest greater access to secondary carbon sources and that sulfate reducers were more reliant on exudates. Soil organic carbon was not the likely secondary source because porewater dissolved inorganic carbon δ^{13} C values did not change during transit through the reactors, despite a ~26% difference between the supplied seawater and marsh soil. Interpretation of oxygen consumption rates is complicated by non-respiratory oxidation of reduced inorganic compounds and possibly significant lithoautotrophy. Exudate pulses elicited rapid and ephemeral respiratory responses, particularly under anoxia, but non-respiratory oxidation of reduced compounds obscured the impact of oxygen availability in our experimental

- system. Despite this, greater aerobic respiration rates suggest that oxygen availability has more
- 45 potential to regulate carbon mineralization in coastal wetlands than root exudates.

1. Introduction

47

48

49

50

51

52

53

54

55

56

57

58

59

60

61

62

63

64

65

66

67

68

69

Accelerating sea-level rise (SLR) threatens the global sustainability of salt marshes (Törnqvist et al., 2021; Saintilan et al., 2022). Two key ecosystem services – carbon sequestration and storm surge buffering – depend upon rapid soil accretion and long-term organic matter preservation. Soil waterlogging and increasingly anoxic conditions thermodynamically constrain decomposition but can increase microbial access to buried organic matter by reducing mineral protection (LaCroix et al., 2019; Huang et al., 2020; 2021). Greater inundation can either stimulate or depress grass productivity and thereby increase or decrease root release of bioavailable carbon compounds (hereafter, exudates) and oxygen. Exudates fuel heterotrophic microbes and may catalyze priming of existing organic matter while oxygen availability lifts thermodynamic barriers to decomposition (Megonigal et al., 2003; Mueller et al., 2016; Jilling et al., 2021). Parsing the effects of root exudates and oxygen availability on heterotrophic respiration and the stability of buried organic matter is difficult because these inputs are ephemeral and spatially variable. However, constraining their individual and combined impacts on soil processes is important for marsh carbon models and predicting future sustainability.

Tidal waters saturate marsh soils, slowing gas exchange with the atmosphere and resulting in a near complete depletion of oxygen within millimeters of the surface. Oxygen delivery below this layer is spatially and temporally variable, depending on porewater flushing, bioturbation, and root release (Kostka et al., 2002a; Koretsky et al., 2008; Koop-Jakobsen et al., 2018). Sporadic oxygen injection creates hotspots of aerobic decomposition (Mueller et al., 2016; Koop-Jakobsen et al., 2018; Bulseco et al., 2020) and oxidation of reduced compounds (Fig. 1) (Giblin and Howarth, 1984; Hyun et al., 2007; Thomas et al., 2014). The latter

regenerates electron acceptors (e.g., SO4²⁻, Fe(III)) that can be subsequently used to oxidize organic matter. Oxygen delivery and rapid consumption create oscillating redox conditions that may further affect decomposition by influencing microbial interactions and mineral-organic matter associations (Aller, 1994; Bhattacharyya et al., 2018; Huang et al., 2020). Through these different mechanisms, the delivery of oxygen into the sub-surface can lead to decomposition of recent organic matter deposited by roots and bioturbators, and carbon buried decades to hundreds of years ago and potentially lessen the strength of the marsh soil carbon sink (Mueller et al., 2016; Luk et al., 2021; Noyce et al., 2023).

70

71

72

73

74

75

76

77

78

79

80

81

82

83

84

85

86

87

88

89

90

91

92

Fractions of recently photosynthesized carbon are released into the rhizosphere where they directly and indirectly stimulate respiration (Fig. 1). Root exudates are rapidly assimilated by microbes (Hines et al., 1989; Megonigal et al., 1999; Spivak and Reeve, 2015), but plant species-specific release rates, composition, and synchrony with oxygen loss are largely unknown (Koretsky et al., 2008; Sutton-Grier and Megonigal, 2011; Zhang et al., 2019). With energy gained from bioavailable exudates, microbes may be able to access older or more complex organic matter (e.g., priming; Blagodatskaya and Kuzyakov, 2008; Mau et al., 2015; Cui et al., 2020). Alternatively, certain compounds in exudates can disrupt mineral-organic matter associations, making formerly protected carbon more vulnerable to microbial attack (Keiluweit et al., 2015; Jilling et al., 2021). Spatial and temporal variability in exudate release create a fluctuating resource environment where microbes must continuously respond or else maintain steady metabolic rates. The former is consistent with a tight dependence of microbes on carbon supplied by plants while the latter might suggest access to another organic matter source that can sustain metabolism between pulses. Such secondary sources of organic matter could include refractory compounds accessed via priming, compounds liberated from mineral associations, and microbial necromass (Cui et al., 2020; Hu et al., 2020). Better understanding microbial responses to deal with changing exudate inputs may provide insight into controls on carbon cycling and storage (Wang et al., 2016; Malik et al., 2020).

We experimentally tested the effects of pulsed, simulated root exudates under oxic and anoxic conditions and whether availability of those resources facilitates mineralization of existing organic matter in mineral wetland soils using flow-through reactors (Roychoudhury et al., 2003; Bulseco et al., 2019). We hypothesized that oxygen availability and carbon exudates combined will stimulate high rates of heterotrophic aerobic respiration and facilitate priming of existing soil organic matter (Fig. 1, left, red processes). Oxygen availability will also support lithotrophic and abiotic oxidation of reduced compounds and recycling of electron acceptors (Fig. 1 left, blue and black processes). Under anoxic conditions, exudates will stimulate sulfate reduction and priming of existing soil organic matter, but to a lesser extent (Fig. 1 right). We further predicted that oscillations in aerobic fluxes would be smaller than anaerobic fluxes (i.e., sulfate reduction) due to greater use of alternate carbon sources (Fig. 1 bottom, right), compared to when microbes are tightly coupled to exudate pulses (Fig. 1 bottom, left). Finally, we expected that cessation of exudate pulses will elicit a more rapid drop in anaerobic respiration rates, due to thermodynamic and kinetic constraints placed by anoxia on access to soil organic matter.

Conceptual diagram of oxygen and carbon availability effects on soil respiration

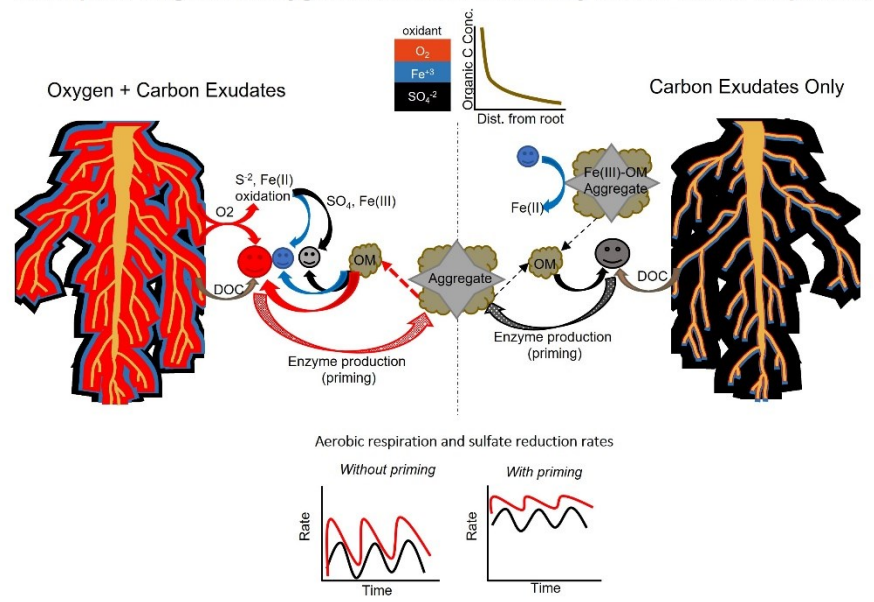


Fig. 1. Conceptual diagram of hypothesized effects of pulsed carbon exudates on microbial respiration and priming of soil organic matter (SOM). (Left) Oxygen and carbon stimulate heterotrophic respiration that, in turn, facilitates SOM priming. Oxygen also supports oxidation of reduced compounds and electron acceptor recycling. (Right) Carbon exudates stimulate sulfate reduction and SOM priming, but to a lesser extent. Reduction of certain minerals provides another OM source for heterotrophs. (Bottom) Predicted aerobic respiration (red) and sulfate reduction (black) rates with (right) and without (left) priming. Roots and soil aggregates are for illustration only and were not included in the experiment. Red, blue, and black processes (arrows) and rhizosphere zones (shading) represent oxygen, iron, and sulfate levels while faces represent dominant pathways of heterotrophic microbial respiration. The size of the shading, arrow, or face reflects relative magnitude. Based on Neubauer et al. 2008, Keiluweit et al 2015, and Spivak et al. 2019. Root image from the IAN library.

2. Materials and methods

125

126

127

128

129

130

131

132

133

134

135

136

137

138

139

140

141

142

143

144

145

146

147

2.1 Experimental design and setup

We experimentally tested how soil microbial communities respond to pulsed inputs of bioavailable compounds under oxic and anoxic conditions. We aimed to assess abiotic processes by reducing microbial activity with the inhibitor sodium azide (NaN₃). Each of four treatments (oxic or anoxic X with or without NaN₃) was replicated three times for a total of 12 experimental units. Soil cores from Spartina alterniflora marshes (9.4 cm diameter x 50 cm deep; 31.42049 °N, 81.29235 °W) and 0.2 µm filtered seawater (30-34 PSU, 2 m depth; 31.319989 °N, 81.178042 °W) were collected from the Georgia Coastal Ecosystems – Long-Term Ecological Research domain during summer 2020. Cores were cut laterally and soils from below the rooting zone at 30-40 cm were removed and used either in the experiment or to determine bulk density. We used soils from below the rhizosphere to assess microbial responses to carbon pulses because this horizon should have more stable environmental conditions and greater isolation from recent root inputs. However this horizon could be influenced by actively growing roots that move soil into the rhizosphere or following changes in environmental conditions that alter root: shoot ratios (e.g., nitrogen loading, warming), plant trait expression, or species composition (Darby and Turner, 2008; Bernal et al., 2016; Noyce and Megonigal, 2021; Mozdzer et al., 2023). Soils for the experiment were cleared of visible roots and rhizomes, mixed, and divided across 12 flow-through reactors (FTR) under a N₂ atmosphere. The FTR design is based on Pallud et al. (2007) as modified by Bulseco et al. (2019) and chosen because it allows for continuous, non-invasive biogeochemical rate measurements without accumulation of metabolic by-products. Each FTR was packed with

31.8 cm³ of field-moist soil sandwiched by pairs of Whatman GF/F and GF/A filters (0.45 and

1.6 μm pore size, respectively) and sealed between radially scored plexiglass ports, designed to promote uniform flow. Six FTRs were maintained in anaerobic chamber (Coy Laboratory Products) with an O₂-free atmosphere (95:5 N₂: H₂) while the other six were maintained in an oxic, ambient atmosphere.

The FTRs were continuously supplied with room temperature, filtered seawater through VitonTM tubing (0.8 mm ID, Cole-Parmer) using Masterflex L/S peristaltic pumps. Target flows of 0.06 mL min⁻¹ simulated in situ soil infiltration rates. Flow conditions were verified using the conservative tracer sodium bromide (Fig. S1). Seawater was maintained in the dark and ammonium, nitrate, and phosphate concentrations were amended to ~57, ~15, and ~35 μM, respectively, to reflect field conditions (Spivak, unpublished), and prevent microbial nutrient limitation. Water for the anoxic treatments was bubbled with N₂ while water for the oxic treatments was not bubbled to maintain ambient gas concentrations. To separate biotic and abiotic processes, water supplying half of the anoxic and oxic treatments was amended with the microbial inhibitor NaN₃ at 5 mM initially, then increased to 10 mM after the first three weeks. The FTRs equilibrated under constant conditions for two weeks before experimental exudate pulses began.

Weekly from Jul 30 - Oct 21, 2020, 23 mL of a 6.76 mM-C cocktail of 3.1% amino acids, 45.7% sugars, and 51.2% organic acids in seawater (Table 1) was pulsed into each FTR. These compounds and concentrations were chosen to mimic root exudates (Kraffczyk et al., 1984), and fall within the range of field porewater observations of 0-20 mM dissolved organic carbon (DOC) at our site (Weston et al., 2006a). The exudate cocktails were degassed with N₂ gas or amended with NaN₃ as required. The experiment continued for 13 days (until Nov 2, 2020) after the final pulse to assess microbial responses to prolonged, low DOC conditions (i.e., starvation).

171 Table 1: Composition of the simulated root exudate cocktail supplied weekly to the FTRs.

Substrate	Fraction (%)	Substrate (µM)	Carbon (µM)	Type	Type Fraction (%)
Glutamic Acid	1.2	15.9	79.5	Amino 3.1 Acid	
Aspartic Acid	0.9	15.7	62.8		3.1
Alanine	1.0	22.1	66.3		
Glucose	21.7	245	1470	Sugar 45.7	
Arabinose	14.6	198	990		45.7
Fructose	9.4	106	636		
Fumaric Acid	35.0	592	2368	Organic 51.2 Acid	
Oxalic acid	12.1	409	818		51.2
Citric Acid	4.0	45.0	270		
Total	100	1648	6761		100

2.2 Metabolism measurements and dissolved phase analyses.

173

174

175

176

177

178

179

180

181

182

183

184

185

186

187

188

189

190

191

192

193

194

195

Soil respiratory responses were measured every two weeks during the pulsing phase of the experiment (days 1-83) and four times following the final pulse (days 84-97). Metabolic rates were measured 1 and 5 days following each pulse to test short-term microbial responsiveness over the experiment. The 1-day time step was based on our expectation of a slightly lagged microbial response and to allow sufficient flushing of the carbon pulses prior to sample collection (~6 FTR turnover times). The 5-day sampling points represented a return to low carbon supply conditions. Paired samples were collected from the seawater reservoirs (i.e., inflow) and the FTR outflows at each time point and analyzed for salinity, pH, and dissolved organic and inorganic carbon (DOC, DIC), dissolved oxygen (DO), and sulfide concentrations. We sought to limit outgassing by minimizing headspace, atmosphere-exposed sample surface area, and collection time. Trace metals were not collected due to resource constraints. Salinity and pH were measured with a handheld refractometer and a benchtop dual channel pH/ISE meter (FisherbrandTM AccumetTM XL250, accuracy ±0.002 pH units) and a calibrated pH combination electrode (FisherbrandTM accuTupHTM), respectively. The DIC and DOC samples were analyzed on a Shimadzu TOC-L. Briefly, the DIC samples were analyzed by acidification with 6 M phosphoric acid and integrating the CO₂ emission peak measured in zero-air carrier gas bubbled through the reaction chamber. Samples were calibrated using an acidified water blank and Dickson CO₂ certified reference material (Dickson et al., 2003). The DOC samples were analyzed by injecting samples onto 460 °C platinum catalyst and integrating the CO₂ emission peak measured in zero-air carrier gas passed through the high-temperature reaction chamber. DIC concentration measured in each sample was subtracted from the raw uncorrected DOC measurements provided by the instrument to calculate the true DOC sample concentration.

Samples were calibrated using a 7-point DOC external standard curve, measured throughout a multi-day automated sample analysis period, approximately one randomly ordered standard after every 7 samples. Dissolved oxygen was measured with an optical DO probe (YSI ProODO). Sulfide samples were stabilized with an antioxidant buffer solution and concentrations were measured with a silver/sulfide ion selective electrode (Spivak et al., 2020). The δ^{13} C composition of DIC in the supply water and FTR outflows was measured after the final pulse, to assess microbial carbon sources, by LC-IRMS (Brandes, 2009). Triplicate 25 μ L subsamples from the experiments were analyzed using a Thermo Scientific Surfveyor HPLC pump/autosampler interfaced with a ThermoScientific LC-Isolink to a Delta V + IRMS. Sodium bicarbonate (NaHCO3) standard solutions, calibrated to the NBS 19 standard, were employed as isotopic references, and all values are reported based on the vPDB standard scale. Typical precision for samples was 0.1%.

2.3 Solid phase analyses

Soil physical properties and geochemical composition were characterized at the beginning and end of the experiment. Bulk density of the 30-40 cm horizon was determined by drying to constant mass at 60 °C. Additional field samples were used to determine soil particle density by measuring the mass of water displaced after adding 25 g of freeze-dried soil to 50 mL. Particle density was calculated as the mass of freeze-dried soil per volume.

Soils collected initially and at the end of the experiment were stored at -80 °C prior to analysis for elemental content and stable isotope composition, acid-hydrolysable carbon and nitrogen, and solid-phase iron concentrations. Samples for elemental and isotopic analyses were dried to constant mass (60 °C), homogenized with a Retsch Mixer Mill 200, and fumed with

hydrochloric (HCl) acid to remove carbonates. Analyses were conducted by the UGA Center for Applied Isotope Studies and data are reported in the conventional δ -notation in units of per mil (‰). All values are reported based on the vPDB standard scale. Acid-hydrolysable carbon and nitrogen were determined by adding 6 N HCl to freeze-dried soils and heating at 105 °C for 2 hours (Silveira et al., 2008). Cooled samples were centrifuged and rinsed four times with Milli Q water. Soils were dried to constant mass, homogenized, and analyzed for elemental and isotopic composition. The acid-hydrolysable fraction was calculated as the difference in carbon content between untreated and acid-treated soils and operationally represents compound classes with faster turnover times (e.g., proteins, nucleic acids, polysaccharides) (Silveira et al., 2008). The residue remaining after hydrolysis includes acid insoluble compounds, such as lignin.

Solid-phase iron was characterized as poorly ordered, organically bound, or crystalline via a sequential extraction of 1 M HCl (poorly ordered), 0.1 M sodium pyrophosphate (pH 10.4; organically bound), and 50 g L⁻¹ sodium dithionite in 0.25 M sodium citrate buffer (pH 4.8; crystalline) (Koretsky et al., 2008; Claff et al., 2010). Soils were rinsed with Milli Q water between each step. Extracts were treated with concentrated HCl and 3 M hydroxylamine HCl and reduced on a hot plate. A 2 mL subsample was treated with 1.2 mL of 3.8 M ammonium acetate buffer, 650 μL 60.5 mM phenanthroline solution, and 6.15 mL Milli Q water. Sample color developed over 24 h prior to absorbance measurements on a Shimadzu UV-1800 spectrophotometer. Concentrations were calculated against a 0-53 μg Fe mL⁻¹ standard curve.

Initial microbial biomass carbon was determined by chloroform fumigation (da Silva et al., 2016). Three of six, 20 g field-moist soil samples were fumed with chloroform in a vacuum desiccator for 72 hours. All six samples were then extracted with 50 mL of 0.5 M potassium sulfate on a shaker for 18 hours in the dark, filtered, and absorbances were measured at 495 nm

on a Shimadzu UV-1800 spectrophotometer against a 0-4 μmol C mL⁻¹ standard curve as described by Bartlett and Ross (1988).

2.4 Microbial inhibitor trials

Because metabolic responses were often similar in treatments with and without NaN₃ we conducted a trial testing whether the inhibitor was quenched by the soil matrix and less effective than the poison mercuric chloride (HgCl₂). The trial included four soil: seawater slurries (no soil, 1:20, 1:4, and 1:1) under three inhibition conditions (no inhibition, 7.5 M NaN₃, and 0.65 M HgCl₂) that were incubated for three time steps (2-, 24-, and 72-hours). Treatments were run in triplicate, under an ambient (oxic) atmosphere, with field moist soil. Slurries were continuously shaken to maintain suspension. Dissolved oxygen concentrations were measured with a ProODO YSI probe.

2.5 Data analyses

Soil metabolism rates were calculated by normalizing concentration differences between the FTR outflows and inlets (i.e., outflow minus inlet), to the soil volume and turnover time of individual reactors (i.e., μ M cm⁻³ h⁻¹). Positive and negative flux rates represent net production or consumption, respectively. Measured DIC rates were compared to rates calculated from stoichiometric equivalents (hereafter as *carbon equivalents*) of oxygen consumption in the aerobic treatments assuming a respiratory quotient of one, and from sulfate reduction as estimated through sulfide production in the anaerobic treatments using a 2:1 molar ratio of carbon mineralized per sulfide produced. Comparisons between measured and calculated (i.e., expected) DIC rates allow us to assess the assumption that aerobic heterotrophy and sulfate

reduction are the dominant metabolisms in the oxic and anoxic treatments, respectively, and to consider alternate processes that could have contributed to discrepancies.

We tested our hypotheses regarding responses to oxygen availability and pulsed carbon inputs with data from the first 84 days of the experiment. Boxplots were used to detect outliers, revealing that metabolic responses during the first 6 days (2 sampling points) were substantially higher than other measurements. We attribute this to a starvation response following the 2-week acclimation period when supply water DOC concentrations were low. Those 2 sampling points were removed from subsequent analyses. Initial data evaluation also revealed that the microbial inhibitor was ineffective in the oxic treatments, thereby preventing assessment of biotic and abiotic controls; treatments receiving NaN₃ were removed from further analyses.

To detect differences in metabolic rates between atmosphere treatments (oxic vs. anoxic) and in response to carbon pulses (day 1 vs. 5), as well as how those effects changed over time, we constructed a series of linear mixed effect models using the nlme package for R (Pinheiro et al., 2016). The mixed models evaluated the fixed effects of atmosphere, immediate- and short-term responses to carbon pulses, and experimental day. Because oxygen consumption and sulfide production rates were negligible or zero in anoxic and oxic treatments, respectively, we used simplified models that excluded the fixed effect of atmosphere for those response variables. When there was a significant interaction (p < 0.05) between response to the carbon pulse and experimental day, the dataset was split into 1- or 5-day response groups and modeled against experimental day, to evaluate how those responses changed over time. For all models, we specified a first-order autoregressive correlation structure to account for our repeated measures sampling design. By modeling covariances among data points sampled within an FTR, a mixed model approach allows us to meet the assumption of independence of errors. For each model, we

calculated the marginal (variance of fixed effects only) and conditional (variance of both fixed and random effects) r² using the piecewiseSEM package in R (Lefcheck, 2016).

Respriatory responses following cessation of carbon pulses were evaluated with data from the 13-day period at the end of the experiment (days 84-97). Changes in metabolic rates over time were modeled as linear or exponential decay relationships, using the lm and nls functions in R. We further evaluated whether pulsed carbon inputs allowed microbes to access existing soil organic carbon by testing for compositional differences in 13 C-DIC between supply water (i.e., inlet) and FTR outflows under oxic and anoxic treatments using similar mixed-effect models. This approach leverages the flow-through experimental design and ~26‰ difference in δ^{13} C signatures between the supplied seawater and marsh soils. We predicted that respiration of marsh soil carbon would substantially reduce the δ^{13} C values of porewater DIC transiting through and exported from the FTRs.

We tested the effects of atmosphere (oxic, anoxic) on soil organic carbon and nitrogen content and isotopic composition and iron phase composition and whether they differed between the beginning and end of the experiment through analysis of variance models (ANOVA).

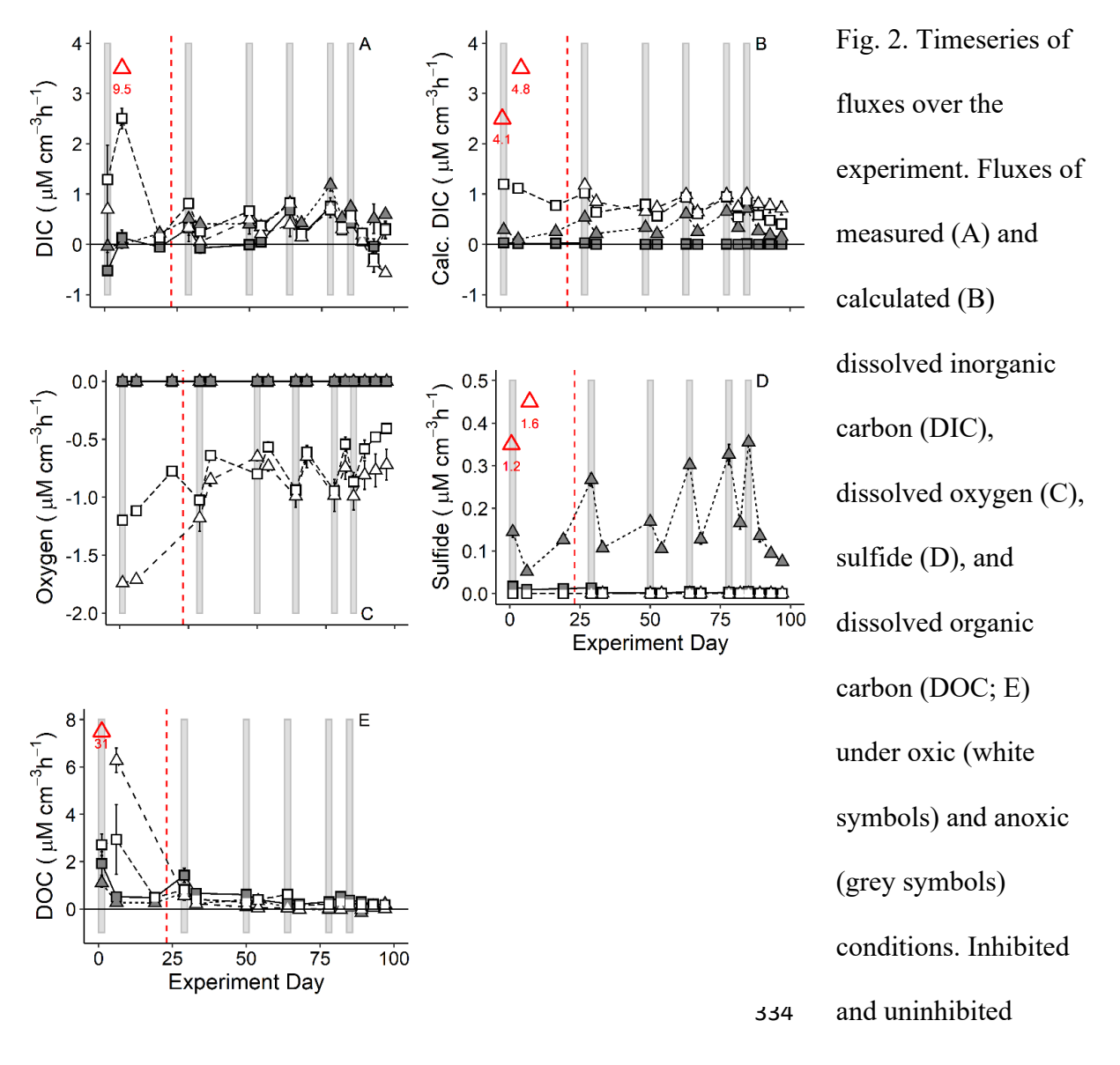
Data were log_{10} -transformed as necessary to maintain homogeneity of variance and values are presented as means \pm standard error (SE), unless noted otherwise. Analyses were performed using R open-source software (R Development Core Team, 2022).

3. Results

3.1 Fluxes following repeated carbon pulses

Fluxes responded strongly to carbon pulses, particularly in the first 6 days of the experiment, and less so to the microbial inhibitor NaN₃, which was much more effective in the

anoxic treatments (Fig. 2). In the microbial inhibitor trials, the effectiveness of both NaN₃ and HgCl₂, as reflected in DO consumption, decreased in slurries with higher proportions of soils, presumably due to dilution (Fig. S2). However, oxygen consumption was similar across control (seawater-only), NaN₃, and HgCl₂ treatments, suggesting that: (1) neither NaN₃ nor HgCl₂ effectively slow or stop microbial respiration in marsh soils or (2) oxygen uptake was dominated by abiotic processes. Because we cannot discern between these possibilities, we focus on the uninhibited treatments from here forward.



treatments are represented by squares and triangles, respectively. Shaded bars indicate rates measured 1 day following carbon pulses. Red dashed lines denote when NaN₃ concentrations were increased. Calculated rates are based on stoichiometric equivalents of oxygen consumption or sulfide production and DIC production. Data from the first 6 days were excluded from statistical analyses due to presumed starvation responses (outliers in red symbols and values). Pulses stopped at day 84 and responses were followed until the end of the experiment.

Metabolism rates were estimated assuming that oxygen and sulfate represented the main electron acceptors in oxic and anoxic treatments, respectively, and that DIC production reflected combined net respiration from all heterotrophic metabolisms (Fig. 2). Oxygen consumption and sulfide production were inhibited under anoxic and oxic conditions and rates slowed by $21 \pm 10\%$ and $55 \pm 8\%$, respectively, between 1- and 5- days following carbon pulses (Figs. 2C-D, 3C-D; Table S1A). Sulfide production rates increased slightly over the middle of the experiment (days 7-84); more so in measurements from 1 day following the pulses compared to 5 days later (Fig. 2D, Table S1B).

341

342

343

344

345

346

347

348

349

350

351

352

353

354

355

356

357

358

359

360

361

362

363

Measured DIC production was faster under anoxic than oxic conditions (Figs. 2A, 3A; Table S1A). This contradicts our expectation that DIC production would be slower in the anoxic treatments, based on assumed thermodynamic constraints and DIC production modeled from stoichiometrically equivalent aerobic respiration and sulfate reduction rates (Fig. 3B; Table S1A). Measured DIC rates slowed between 1- and 5- days following carbon pulses in both oxic and anoxic treatments (Fig. 3A; Table S1). The magnitude of the decrease in anoxic treatments $(52 \pm 17\%)$ was similar to drops in sulfide production (Fig. 3D). However, in the oxic treatment the decline in measured DIC was much greater ($69 \pm 24\%$) than changes in oxygen consumption rates (Figs. 3A, C). Sulfate reduction as the main pathway of anaerobic metabolism is consistent with nearly equivalent measured and calculated DIC rates in the anoxic treatments (Fig. 4) and positive correlations between measured DIC and sulfide production at approximately the expected stoichiometric ratio of 2 (slope 2.38 ± 0.44 , p < 0.001, $r^2 = 0.48$). However, in the oxic treatments imbalances between measured and calculated DIC rates (Fig. 4) and a lack of correlation between oxygen consumption and DIC production indicate that processes other than aerobic respiration influenced these dynamics. The effects of respiration on the carbonate system were reflected in outflow water pH levels, which were 0.49 ± 0.04 and 0.23 ± 0.03 units lower than the supply water in the oxic and anoxic treatments, respectively.

Dissolved organic carbon fluxes were generally positive and similar in oxic and anoxic treatments but slowed over the course of the experiment (Figs. 2E, 3E; Table S1). Rates were slightly higher 1 day following carbon pulses compared to 5 days later; this likely reflects a biological response since day 1 rates were measured after ~6 FTR turnovers following the pulse (Fig. 3E Table S1). These results are consistent with microbes responding quickly to inputs of bioavailable compounds by producing DOC. Further compositional analyses would be useful in characterizing the dissolved organic matter rapidly produced and released by microbes.

3.2 Two weeks after the last carbon pulse

Flux rates slowed over the 2-week period following the final carbon pulse; however, DIC, DOC, dissolved oxygen, and sulfide followed different trajectories (Fig. 5; Table S2). Dissolved oxygen consumption slowed by ~28%, with the sharpest change between days 1 and 5 (Fig. 5C). Sulfide production rates were more sensitive to the cessation of pulses, dropping ~78% and following an exponential decay (Fig. 5D). Surprisingly, measured DIC fluxes did not clearly follow changes in oxygen consumption and sulfide production (Fig. 5A). In the oxic treatments, DIC rates decreased linearly and, by day nine, switched from net production to uptake. In the anoxic treatments, DIC fluxes fell by ~19%, a far smaller change than in sulfide production. Flux rates of DOC did not follow clear trends in either oxic or anoxic treatments (Fig. 5E). Despite the different trends, slowing rates are consistent with primarily biotic controls on fluxes and microbial reliance on new carbon inputs rather than a shift to soil-associated organic matter.

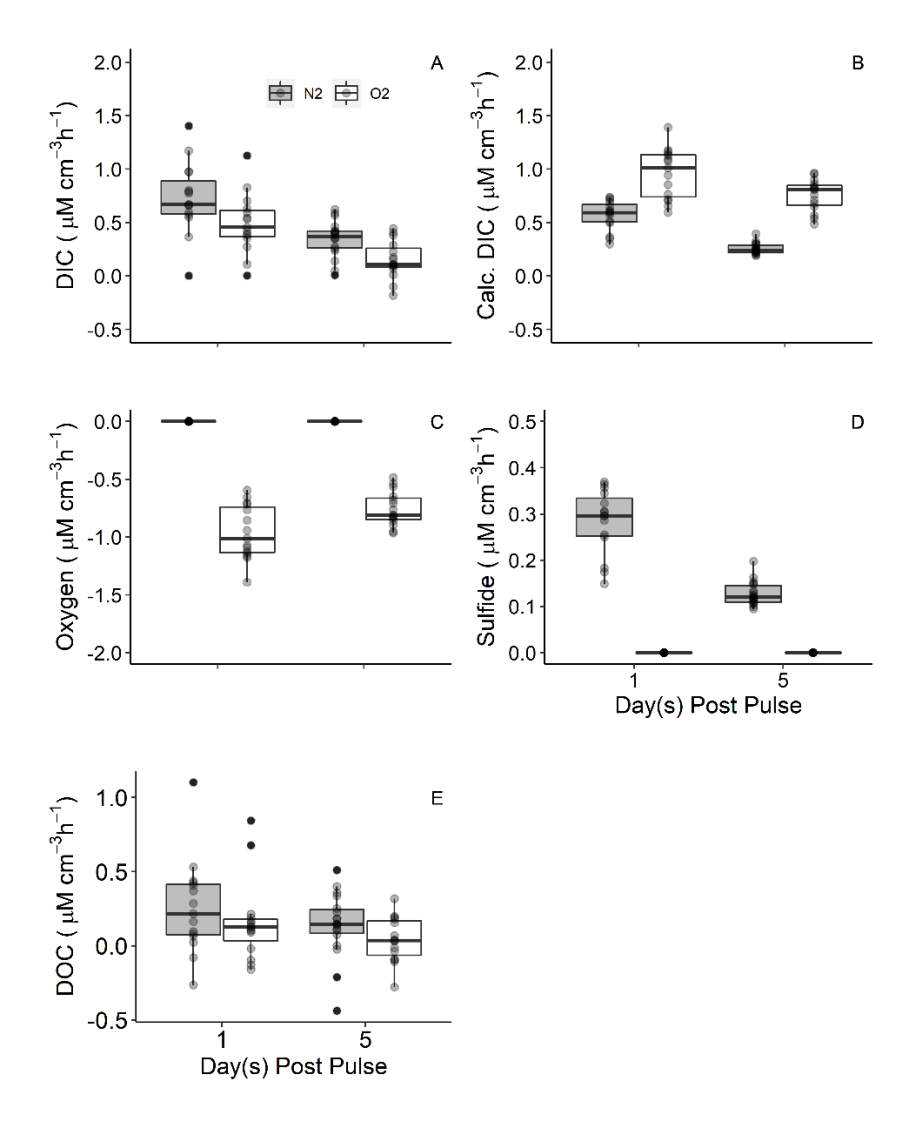


Fig. 3. Fluxes aggregated by 1 or 5 days following carbon pulses. Box and whisker plots of measured (A) and calculated (B) dissolved inorganic carbon (DIC), dissolved oxygen (C), sulfide (D), and dissolved organic carbon (DOC; E) fluxes aggregated by one vs. five days following organic carbon pulses. Grey boxes are anoxic while white boxes are oxic treatments. See Table S1 for statistical results.

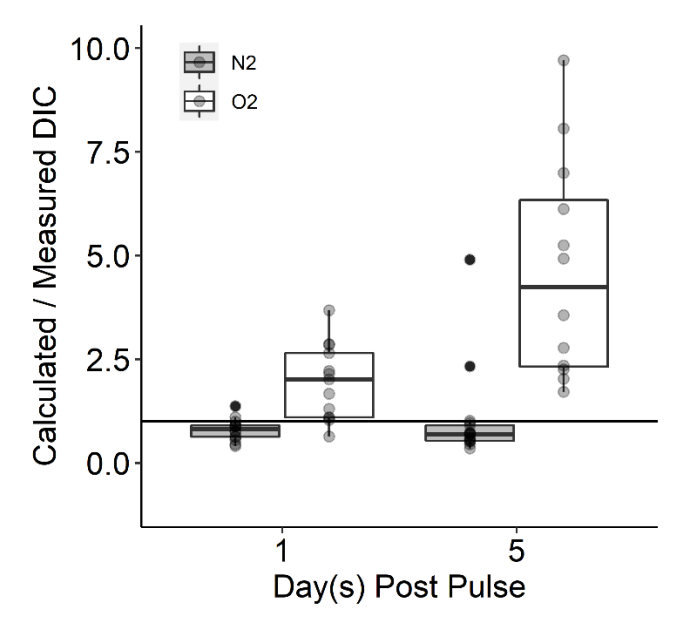


Fig. 4. Calculated-to-measured dissolved inorganic carbon (DIC) fluxes on 1 or 5 days following the pulses. Calculated rates are based on stoichiometric equivalents of oxygen consumption or sulfide production and DIC production. The horizontal line represents a 1:1 ratio that would be expected if the calculated and measured DIC rates were equal such that either aerobic respiration (oxic treatment, white boxes) or sulfate reduction (anoxic treatment, grey boxes) accounted for all or nearly all DIC production.

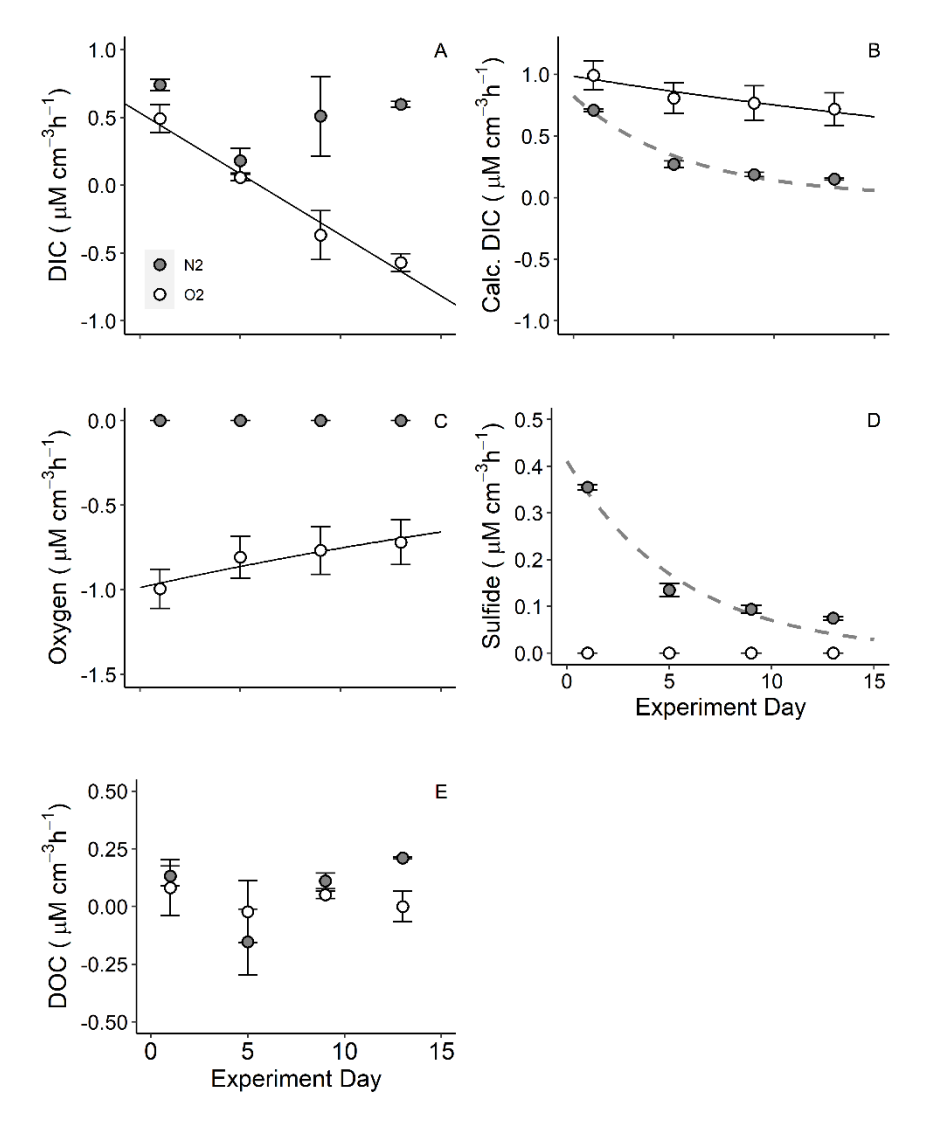


Fig. 5. Fluxes after the final carbon pulse. Fluxes of measured (A) and calculated (B) dissolved inorganic carbon (DIC), dissolved oxygen (C), sulfide (D), and dissolved organic carbon (DOC, E) under oxic (white symbols) and anoxic (grey symbols) conditions in the 13 days following the final carbon pulse. Solid black and dashed grey lines reflect statistically significant (p<0.05) correlations in oxic and anoxic treatments respectively. Data are mean +/- SE. See Table S2 for coefficient values.

3.3 Soil composition

Soil elemental content and isotopic composition were insensitive to the experimental treatments (Fig. S3; Table S3). Total organic carbon and nitrogen content were similar between pre-experiment soils and those collected at the end from the oxic and anoxic treatments. Likewise, δ^{13} C and δ^{15} N did not vary between treatments. Acid hydrolysis released ~4% of carbon from soils collected at the beginning and end of the experiment, and from oxic and anoxic treatments. Iron composition was dominated by crystalline minerals with lower levels of poorly ordered and organic-bound phases. Soil iron composition was similar at the beginning and end of the experiment, except for a slight decrease in poorly ordered minerals (e.g., sulfides, oxides), and between oxic and anoxic treatments (Fig. S3; Table S3).

4. Discussion.

4.1 Does oxygen availability regulate soil respiration?

Exposing soils from below the rooting zone to oxygen produced carbon fluxes that were both consistent and inconsistent with a tenet of wetland science: increasing availability of oxygen and other electron acceptors accelerates decomposition in saturated belowground environments (Kristensen et al., 1995; Mueller et al., 2016; Bulseco et al., 2019). When microbial respiration was approximated from oxygen and sulfide fluxes (i.e., as carbon equivalents), oxic rates were $41 \pm 10\%$ to $66 \pm 7\%$ greater than anoxic rates (Figs. 2B-D; 3B-D). However, measured DIC fluxes were $33 \pm 21\%$ to $56 \pm 25\%$ faster under anoxic vs. oxic conditions (Figs. 2A, 3A). These contrasting responses highlight the complexities of interacting heterotrophic and autotrophic redox-sensitive metabolisms and abiotic processes that can decouple oxygen and carbon dynamics.

Sulfate reduction was the primary, but unlikely the only, heterotrophic metabolism under continuously anoxic conditions based on the calculated (2.38 \pm 0.44) and theoretical stoichiometries of DIC to sulfide production. Iron cycling can be substantial in Georgia's salt marshes and would affect net DIC and sulfide fluxes but was not characterized here (Kostka et al., 2002b; Hyun et al., 2007; Kolton et al., 2020). Dominance by sulfate reduction is expected from the high sulfate concentration of estuarine waters percolating through most salt marsh soils (Howarth and Giblin, 1983; Kostka et al., 2002b; Hyun et al., 2007). Rates of sulfide production were comparable to sulfate reduction under more natural conditions when experimental inputs of bioavailable carbon were low (e.g., 9 days after the last pulse; Fig. 5D) (Howarth and Giblin, 1983; Kostka et al., 2002b; Roychoudhury et al., 2003). In the oxic treatments, net sulfide production was only apparent in the two sampling points following the acclimation period and initiation of carbon pulses (Fig. 2D). The first carbon pulse resulted in oxygen depletion to 16-39 percent saturation, thereby facilitating conditions that favor anaerobic microsites and net sulfide production (Fig. 2D). Outflow oxygen concentrations did not drop to such low levels again; however, given that outflow water was typically near the threshold for hypoxia it is likely that sulfate reduction occurred throughout the oxic experiment, but sulfides were oxidized or consumed within the FTRs. Our estimates of sulfate reduction are likely conservative because they are based on the production of sulfide, which is readily oxidized under oxic conditions and consumed via reduction of Fe(III) minerals in anoxic soils (Luther et al., 1982; Giblin and Howarth, 1984; Mortimer et al., 2011). Pairing sulfide with sulfate measurements and complementary characterization of other biotic and abiotic pathways would be needed to better ascertain contributions from different heterotrophic metabolisms.

434

435

436

437

438

439

440

441

442

443

444

445

446

447

448

449

450

451

452

453

454

Faster carbon-equivalent rates of oxygen consumption than sulfide production indicate that microbial communities sampled from continuously anoxic soils (i.e., below roots, rhizomes, and burrows), include members that are readily able to conduct aerobic respiration. The simple sugars, amino acids, and organic acids making up the carbon pulses should have been accessible directly to aerobes and indirectly to sulfate reducers following fermentation (Table 1) (Muyzer and Stams, 2008; Lin et al., 2021), but higher oxygen consumption rates in the oxic treatment suggest that aerobic microbes responded more quickly to capitalize on the added carbon (Kristensen et al., 1995; Kristensen and Holmer, 2001). The difference between carbonequivalent oxygen and sulfide rates unexpectedly increased five days after the carbon pulses ended (Fig. 3B, Table S1A). This could suggest that aerobes were better able to use more refractory or mineral-associated organic matter when inputs of bioavailable carbon were low, which is expected considering energetic limitations on the mineralization of complex organic compounds in the absence of oxygen (Keiluweit et al., 2016) and consistent with more extensive degradation of terrestrial organic matter in estuary and nearshore sediments when oxygen exposure times are longer (Hedges and Keil, 1995; Spivak, 2015). Faster bacterial turnover under oxic conditions and immobilization of soil nitrogen (i.e., lower C:N; Table S3; Fig. S3) could have also contributed to higher aerobic respiration between carbon pulses (Sun et al., 2002; Simpson et al., 2007; Cui et al., 2020). Alternatively, a substantial fraction of oxygen consumption may have been driven by non-respiratory oxidation of reduced compounds (Giblin and Howarth, 1984; Kostka et al., 2002a; Luther et al., 2011; Jørgensen et al., 2019).

456

457

458

459

460

461

462

463

464

465

466

467

468

469

470

471

472

473

474

475

476

477

478

Aerobic respiration and non-respiratory oxidation of reduced inorganic compounds likely explain faster rates of oxygen consumption than sulfide production and discrepancies between measured and calculated DIC rates (Figs. 3A-B, 4). It is unlikely that the stoichiometric

imbalance between oxygen consumption and DIC production (Fig. 4) was due to inorganic carbon removal via precipitation since siderite (FeCO₃) requires reduced iron and anoxic conditions (Lin et al., 2020) and porewaters at Sapelo Island are undersaturated with respect to carbonate minerals (Giblin and Howarth, 1984). However, comprehensive measurements of inorganic carbon and metal ion concentrations and total alkalinity would be required to calculate ion activity products and assess the potential role of mineral precipitation. Oxidation of reduced inorganic compounds (e.g., H₂S, iron monosulfides) would have inflated calculated DIC rates because we assumed oxygen was only consumed by aerobic respiration, with a respiratory quotient of one. Metabolic pathways coupling oxidation of reduced compounds to carbon fixation may also explain lower rates of measured DIC production under oxic conditions (Fig. 3A). For instance, sulfur oxidizing bacteria are abundant in salt marsh soils, including in Georgia, and many fix inorganic carbon into biomass (Wirsen et al., 2002; Thomas et al., 2014; Rolando et al., 2022). Thus, it is likely that respiration rates were faster under oxic conditions, but inorganic carbon uptake by sulfur oxidizers resulted in slower measured DIC rates, which is consistent with a lack of correlation between oxygen and DIC. An alternative explanation is that the faster measured DIC production rates in the anoxic treatments are real and reflect liberation of bioavailable carbon following reductive dissolution of iron oxide minerals (Bhattacharyya et al., 2018; Huang et al., 2020; Huang et al., 2021). Misattributing oxygen consumption and underestimating DIC production likely explain higher calculated vs. measured DIC rate ratios, particularly at the day 5 time points when heterotrophic oxygen demand (i.e., respiration) decreased, but further constraining oxygen effects on carbon mineralization requires better estimation of sulfur and perhaps iron cycling.

27

501

479

480

481

482

483

484

485

486

487

488

489

490

491

492

493

494

495

496

497

498

499

4.2 Responses to fluctuating carbon inputs

Rhizodeposition is spatially and temporally variable, creating a constantly changing environment for soil microbes (Cardon and Gage, 2006; Koop-Jakobsen et al., 2018; Pett-Ridge et al., 2021). Microbial communities respond rapidly to oscillating redox conditions (Sundby et al., 2003; Bhattacharyya et al., 2018; Spivak et al., 2020) and new organic matter inputs (Megonigal et al., 1999; Koretsky et al., 2003; Spivak and Reeve, 2015), but it is less clear whether they acclimate and sustain optimal metabolic rates when resources fluctuate or continually adapt. Our experiment demonstrates that microbes in wetland soils with relatively low organic carbon content are opportunistic and capitalize on pulses of bioavailable compounds rather than maintain more constant rates through various mechanisms when resources are low (Figs. 2, 3, 5).

Pore water DOC levels in Georgia salt marshes vary seasonally and can range from a couple- to tens- of millimolar (Weston et al., 2006a; Weston et al., 2006b). The DOC concentrations of the South Atlantic Bight water supplied to the FTRs were within this range (1.9 \pm 0.01 mM), but perhaps lower than is typical of horizons below the rooting zone. Pulsed carbon additions (6.76 mM) resulted in faster sulfide production rates than measured in the field (Kostka et al., 2002b; Roychoudhury et al., 2003). The rapid and proportionately higher response to moderate DOC levels in our experiment suggests that natural pore waters are rich in complex macromolecules (Zhang et al., 2019) of which a small fraction is bioavailable. Comparing the molecular composition of DOC in FTR supply water and outflows could address this question and provide novel insight into microbial metabolic efficiencies and carbon transformations.

Flux rates fell by about half between one- and five- days following carbon pulses in anoxic treatments, and by $21 \pm 10\%$ to $69 \pm 24\%$ in the oxic treatments, based on oxygen

consumption and DIC production rates, respectively (Figs. 3A, C, D). Consistent differences between one- and five- day rates suggest that rapid microbial responses to carbon inputs may be predictable (Figs. 2, 3). Mass balance and stable isotope tracer approaches could be used to better quantify microbial efficiencies and responses to carbon inputs but require greater sampling resolution before, during, and after carbon pulses. For instance, it is unclear whether day one measurements reflect maximum rates because we do not know the time lag between when microbes detect bioavailable carbon and then upregulate metabolism. Predicting soil microbial respiration would require further deriving relationships between carbon demand and bioavailable inputs as well as characterizing rates, drivers, and composition of tidal wetland root exudates under experimental and natural conditions.

Repeatable responses to DOC pulses suggest that soil microbial communities below the rhizosphere include members that can capitalize on resources that are spatially and temporally heterogeneous. Quick and substantial respiratory responses to changing resource availability also suggest that this is an energetically efficient strategy. Such opportunistic responses are consistent with marsh soils having high microbial diversity, but a small fraction of active taxa (Bowen et al., 2012; Kearns et al., 2016). The slight, but significant, increases in measured DIC and sulfide production rates over time (Table S1B) may further suggest acclimation or anticipatory responses to shifting resource availability and, potentially, more efficient resource capture (Malik et al., 2020). Pairing metabolic rates with microbial community composition and activity using 'omics approaches and stable isotope tracers would be valuable in directly testing these hypotheses. Better understanding microbial life history strategies could provide important new insight into carbon preservation mechanisms in ever-changing salt marsh soil environments and

potentially facilitate integration of these systems into larger-scale, trait-based soil carbon models (Wieder et al., 2013; Spivak et al., 2019; Malik et al., 2020).

4.3. Carbon pulses did not have priming effects

Certain low molecular weight organic compounds released by roots can be assimilated by microbes and may indirectly increase the vulnerability of older SOC to decomposition via priming (Fontaine et al., 2007; Klotzbücher et al., 2011; Keiluweit et al., 2015). Priming is hypothesized to occur through biotic mechanisms, whereby bioavailable root exudates enhance microbial activity and support mineralization of SOC (Klotzbücher et al., 2011), and abiotic mechanisms, in which exudates disrupt mineral-associated organic matter, thereby making it available to microbes for decomposition (Keiluweit et al., 2015; Jilling et al., 2021). However, while microbes responded quickly and repeatedly to the simulated exudate pulses there is little evidence that existing SOC supported respiration.

Following the final DOC pulse, metabolic rates dropped quickly and then plateaued to lower levels within two weeks (Fig. 5C, D; Table S2). Sulfide production under anoxic conditions fell by \sim 78% while measured DIC fluxes dipped but rebounded to within 19% of day one rates (Figs. 5A, D). Consequently, the ratio of measured DIC-to-sulfide rates increased from 1.04 ± 0.07 to 4.01 ± 0.21 , indicating that the contribution of sulfate reduction to soil respiration decreased and other electron acceptors (e.g., Fe) became increasingly important (Bulseco et al., 2019). The carbon sources supporting the rebound in DIC rates are ambiguous. Reduction of iron oxides and dissolution of metal-organic matter complexes by ligands, such as oxalic acid in the carbon pulses, could have made mineral-associated carbon more available to microbes (Luther et al., 1992; Keiluweit et al., 2015; Bhattacharyya et al., 2018; Jilling et al., 2021). However,

similar δ^{13} C-DIC values in FTR supply water and outflows (p > 0.05; data not shown) point to minimal respiration of existing SOC. Alternatively, respiration could have been supported by turnover of microbial necromass (Hu et al., 2020). Regardless, changes in the DIC : sulfide ratio point to either rapid shifts in the composition of the entire microbial community or the taxa that were metabolically active.

570

571

572

573

574

575

576

577

578

579

580

581

582

583

584

585

586

587

588

589

590

591

592

Oxygen availability resulted in sharply different responses in oxygen consumption and DIC production following the final pulse: oxygen consumption in the oxic treatment decreased exponentially to a near constant rate while measured DIC in the oxic treatment decreased linearly (Table S2; Figs. 5A, C). The 28% decrease in oxygen consumption rates could suggest that microbes switched to less bioavailable carbon sources by using soil organic matter, but again, this is not consistent with δ^{13} C- DIC results. Instead, moderate rates of ongoing oxygen consumption without DIC generation likely reflect both turnover (but not mineralization) of microbial biomass and oxidation of reduced sulfur and iron compounds. Oxidation of reduced compounds coupled to carbon fixation in lithotrophic organisms results in DIC uptake but not necessarily oxygen consumption (Canfield, 1989; Schippers and Jørgensen, 2002; Jørgensen et al., 2019). Assuming that: (i) net DIC fluxes reflect the balance between aerobic respiration and lithoautotrophic production, (ii) oxygen was only consumed by heterotrophs, and (iii) a respiratory quotient of one, we estimate lithoautotrophic production as -2.6 to -3.0 µM C g⁻¹ dry soil h⁻¹ on days 9 and 13, respectively, following the final carbon pulse (Fig. 5A, C). This means that carbon uptake was 59-64% of the gross DIC flux and 48-79% greater than aerobic respiration on days 9 and 13, respectively. These are likely lower bounds because our assumptions exclude aerobic chemoautotrophy and the experiment ended before DIC fluxes reached an asymptote. These data highlight the potential magnitude of microbial carbon fixation,

particularly when inputs of bioavailable carbon are low, and the importance of using multiple variables to infer metabolic processes in marsh soils with redox gradients. Moreover they are consistent with low respiratory quotients (~0.5) that demonstrate greater carbon dioxide production than oxygen consumption during the low productivity months of February and October in the surrounding Duplin River-marsh estuary system (Wang et al., 2018).

593

594

595

596

597

598

599

600

601

602

603

604

605

606

607

608

609

610

611

612

613

614

615

Regular pulses of bioavailable carbon compounds stimulate priming in terrestrial soils (Mau et al., 2015) but did not result in respiration of soil organic carbon in our experiment (Fig. S3). The amount of carbon added per pulse was ~91% of microbial biomass carbon (data not shown), which is a comparable ratio to terrestrial experiments reporting strong priming effects (Cui et al., 2020). Respiration of the soil organic carbon in the FTRs (δ^{13} C: -26.83 \pm 0.11 %) should have resulted in a shift in outflow δ^{13} C-DIC to more negative values. Instead, the δ^{13} C-DIC of the seawater supplied to the FTRs (-0.60 ± 0.20 % to 0.35 ± 0.21 %) was statistically similar to outflow water from the oxic (-0.69 \pm 0.07 ‰, p = 0.73) and anoxic (0.17 \pm 0.08 ‰, p = 0.43) treatments in the ~2-weeks following the 13th and final DOC pulse. Substantial shifts in δ^{13} C-DIC values have been observed in similar incubation experiments (Komada et al., 2012) and we expected that respiration of soil organic carbon would increase with each successive DOC pulse and be greatest during the starvation period after the last pulse. The insensitivity of δ¹³C-DIC could suggest that soil-associated organic matter is tightly bound and unavailable to microbes. This would be consistent with a terrestrial origin of soil organic carbon, as indicated by depleted δ^{13} C values (Fig. S3), and extensive oxygen exposure that would have occurred during transit in the Altamaha River prior to deposition in the marsh. However, δ^{13} C -DIC is influenced by a range of processes including sulfur cycling, selective decomposition, fractionation during organic matter oxidation, carbonate dissolution and reprecipitation, and

isotope exchange between CO₂(aq) and carbonates that could complicate interpretation (Hu and Burdige, 2007; Walter et al., 2007; Spivak et al., 2018). Detailed molecular characterization of soils before and after the experiment as well as compound-specific isotope analyses of microbial biomarkers would be needed to more definitively detect compositional changes associated with carbon priming and microbial assimilation.

4.4 Potential priming effects of oxygen pulses

Oxygen priming in a phenomenon that can occur in anaerobic soils and sediments when a perturbation increases oxygen availability, stimulating energetically efficient aerobic respiration and SOC decomposition (Wolfe et al., 2007). While there is compelling evidence of plant-mediated oxygen priming (Mueller et al., 2016; Noyce et al., 2023), in practice it is difficult to quantify the relative contributions of carbon and oxygen priming because wetland plants are sources of both substrates. Our FTR experimental design provides insight into these two processes that both scale with plant biomass but operate by distinctly different mechanisms.

Assuming our calculated DIC production estimates more closely reflect organic carbon mineralization rates, there is greater potential for oxygen priming than carbon priming in the salt marsh soils used in this study. Although we did not observe priming of stable SOC, it may have become apparent if the perturbations persisted for periods greater than in the present study.

5. Conclusions

Microbial communities persisting below the marsh rhizosphere, where the environment is anoxic and stable for decades-to-hundreds of years, are nimble and respond rapidly to changing redox conditions and carbon inputs (Fig. 2). Microbes up-and-down regulate metabolism

predictably according to resource availability and may acclimate over time (Fig. 2; Table S1B). Introducing oxygen substantially increased soil respiration rates but pulses of bioavailable carbon compounds had a greater stimulatory effect under anoxia (Fig. 3B). More muted oscillations in aerobic respiration could suggest greater access to a secondary carbon source (e.g., soil associated carbon, microbial necromass) and that sulfate reducing bacteria are more reliant on root exudates. Yet, non-respiratory oxidation of reduced inorganic compounds complicates interpretation of oxygen fluxes and neither oxic conditions nor carbon pulses resulted in measurable respiration of soil organic carbon (Fig. S3). The latter suggests that short-term disturbances to mineral wetland soils that alter redox conditions may not trigger loss of soilassociated carbon and raises new questions as to why it mainly derives from terrestrial sources rather than autochthonous marsh production (Fig. S3). Our results highlight that estimating oxygen effects on soil metabolism requires constraining multiple interacting biogeochemical cycles that mineralize organic carbon and catalyze the release of energy stored in reduced compounds to fix carbon. This experiment provides new insight into the singular and dual controls of oxygen and carbon inputs on soil processes and hints at underlying biogeochemical mechanisms that could be further tested by characterizing compositional changes in inorganic porewater chemistry, DOC, and active microbial communities. Parlaying mechanisms into natural salt marshes would advance understanding of plant-microbe-mineral-organic matter interactions and predictions of ecosystem responses to future disturbances.

658

659

660

661

639

640

641

642

643

644

645

646

647

648

649

650

651

652

653

654

655

656

657

Acknowledgements

Thanks to A. Bulseco and J. Bowen for guidance in setting up, maintaining, and sampling the experiments. We also appreciate many helpful conversations with J. Bowen, A. Giblin, Z.

662	Cardon, and J. Pett-Ridge. This research was supported by the National Science Foundation
663	(DEB-2121019 and OCE-1832178). The authors declare no competing interests.
664	
665	Data availability.
666	Data are archived with the GCE-LTER project and Environmental Data Initiative
667	(http://dx.doi.org/10.6073/pasta/c6adc3e855ed0d3f66626e4de3ed0616).
668	
669	Author contributions.
670	AP, ACS, and JPM designed the study. AP conducted the research and AP, CH, and JB analyzed
671	the samples. ACS and AP analyzed the data and wrote the manuscript drafts; all authors
672	contributed to editing.

- 673 Literature cited.
- Aller, R.C., 1994. Bioturbation and remineralization of sedimentary organic matter Effects of
- 675 redox oscillation. Chemical Geology 114, 331-345.
- Bartlett, R.J., Ross, D.S., 1988. Colorimetric Determination of Oxidizable Carbon in Acid Soil
- 677 Solutions. Soil Science Society of America Journal 52, 1191-1192.
- Bernal, B., McKinley, D.C., Hungate, B.A., White, P.M., Mozdzer, T.J., Megonigal, J.P., 2016.
- 679 Limits to soil carbon stability; Deep, ancient soil carbon decomposition stimulated by new labile
- organic inputs. Soil Biology and Biochemistry 98, 85-94.
- Bhattacharyya, A., Campbell, A.N., Tfaily, M.M., Lin, Y., Kukkadapu, R.K., Silver, W.L., Nico,
- P.S., Pett-Ridge, J., 2018. Redox Fluctuations Control the Coupled Cycling of Iron and Carbon
- in Tropical Forest Soils. Environmental Science & Technology 52, 14129-14139.
- Blagodatskaya, E., Kuzyakov, Y., 2008. Mechanisms of real and apparent priming effects and
- their dependence on soil microbial biomass and community structure: critical review. Biology
- 686 and Fertility of Soils 45, 115-131.
- Bowen, J.L., Morrison, H.G., Hobbie, J.E., Sogin, M.L., 2012. Salt marsh sediment diversity: a
- test of the variability of the rare biosphere among environmental replicates. The Isme Journal 6,
- 689 2014.
- Brandes, J.A., 2009. Rapid and precise δ13C measurement of dissolved inorganic carbon in
- 691 natural waters using liquid chromatography coupled to an isotope-ratio mass spectrometer.
- Limnology and Oceanography: Methods 7, 730-739.
- Bulseco, A.N., Giblin, A.E., Tucker, J., Murphy, A.E., Sanderman, J., Hiller-Bittrolff, K.,
- Bowen, J.L., 2019. Nitrate addition stimulates microbial decomposition of organic matter in salt
- 695 marsh sediments. Global Change Biology 25, 3224-3241.

- 696 Bulseco, A.N., Vineis, J.H., Murphy, A.E., Spivak, A.C., Giblin, A.E., Tucker, J., Bowen, J.L.,
- 697 2020. Metagenomics coupled with biogeochemical rates measurements provide evidence that
- 698 nitrate addition stimulates respiration in salt marsh sediments. Limnology and Oceanography 65,
- 699 S321-S339.
- 700 Canfield, D.E., 1989. Sulfate reduction and oxic respiration in marine sediments: implications
- 701 for organic carbon preservation in euxinic environments. Deep Sea Research Part A.
- 702 Oceanographic Research Papers 36, 121-138.
- Cardon, Z.G., Gage, D.J., 2006. Resource exchange in the rhizosphere: Molecular tools and the
- microbial perspective. Annual Review of Ecology, Evolution, and Systematics 37, 459-488.
- Claff, S.R., Sullivan, L.A., Burton, E.D., Bush, R.T., 2010. A sequential extraction procedure for
- acid sulfate soils: Partitioning of iron. Geoderma 155, 224-230.
- 707 Cui, J., Zhu, Z., Xu, X., Liu, S., Jones, D.L., Kuzyakov, Y., Shibistova, O., Wu, J., Ge, T., 2020.
- 708 Carbon and nitrogen recycling from microbial necromass to cope with C:N stoichiometric
- imbalance by priming. Soil Biology and Biochemistry 142, 107720.
- da Silva, A.O., Silva, W.M., Kurihara, C.H., Mercante, F.M., 2016. Spectrophotometric method
- 711 for quantification of soil microbial biomass carbon. African Journal of Biotechnology 15, 565-
- 712 570.
- 713 Darby, F.A., Turner, R.E., 2008. Effects of eutrophication on salt marsh root and rhizome
- biomass accumulation. Marine Ecology Progress Series 363, 63-70.
- Dickson, A.G., Afghan, J.D., Anderson, G.C., 2003. Reference materials for oceanic CO2
- analysis: a method for the certification of total alkalinity. Marine Chemistry 80, 185-197.
- Fontaine, S., Barot, S., Barré, P., Bdioui, N., Mary, B., Rumpel, C., 2007. Stability of organic
- carbon in deep soil layers controlled by fresh carbon supply. Nature 450, 277-280.

- Giblin, A.E., Howarth, R.W., 1984. Porewater evidence for a dynamic sedimentary iron cycle in
- salt marshes. Limnology and Oceanography 29, 47-63.
- Hedges, J.I., Keil, R.G., 1995. Sedimentary organic matter preservation: An assessment and
- speculative synthesis. Marine Chemistry 49, 81-115.
- Hines, M.E., Knollmeyer, S.L., Tugel, J.B., 1989. Sulfate reduction and other sedimentary
- biogeochemistry in a northern New England salt marsh. Limnology and Oceanography 34, 578-
- 725 590.
- Howarth, R.W., Giblin, A., 1983. Sulfate reduction in the salt marshes at Sapelo Island, Georgia.
- 727 Limnology and Oceanography 28, 70-82.
- Hu, X., Burdige, D.J., 2007. Enriched stable carbon isotopes in the pore waters of carbonate
- sediments dominated by seagrasses: Evidence for coupled carbonate dissolution and
- reprecipitation. Geochimica Et Cosmochimica Acta 71, 129-144.
- Hu, Y., Zheng, Q., Noll, L., Zhang, S., Wanek, W., 2020. Direct measurement of the in situ
- decomposition of microbial-derived soil organic matter. Soil Biology and Biochemistry 141,
- 733 107660.
- Huang, W., Wang, K., Ye, C., Hockaday, W.C., Wang, G., Hall, S.J., 2021. High carbon losses
- from oxygen-limited soils challenge biogeochemical theory and model assumptions. Global
- 736 Change Biology 27, 6166-6180.
- Huang, W., Ye, C., Hockaday, W.C., Hall, S.J., 2020. Trade-offs in soil carbon protection
- mechanisms under aerobic and anaerobic conditions. Global Change Biology 26, 3726-3737.
- Hyun, J.-H., Smith, A.C., Kostka, J.E., 2007. Relative contributions of sulfate- and iron(III)
- reduction to organic matter mineralization and process controls in contrasting habitats of the
- 741 Georgia saltmarsh. Applied Geochemistry 22, 2637-2651.

- Jilling, A., Keiluweit, M., Gutknecht, J.L.M., Grandy, A.S., 2021. Priming mechanisms
- 743 providing plants and microbes access to mineral-associated organic matter. Soil Biology and
- 744 Biochemistry 158, 108265.
- Jørgensen, B.B., Findlay, A.J., Pellerin, A., 2019. The Biogeochemical Sulfur Cycle of Marine
- 746 Sediments. Frontiers in Microbiology 10.
- Kearns, P.J., Angell, J.H., Howard, E.M., Deegan, L.A., Stanley, R.H.R., Bowen, J.L., 2016.
- Nutrient enrichment induces dormancy and decreases diversity of active bacteria in salt marsh
- sediments. Nature Communications 7, 12881.
- Keiluweit, M., Bougoure, J.J., Nico, P.S., Pett-Ridge, J., Weber, P.K., Kleber, M., 2015. Mineral
- protection of soil carbon counteracted by root exudates. Nature Climate Change 5, 588-595.
- Keiluweit, M., Nico, P.S., Kleber, M., Fendorf, S., 2016. Are oxygen limitations under
- recognized regulators of organic carbon turnover in upland soils? Biogeochemistry 127, 157-
- 754 171.
- Klotzbücher, T., Kaiser, K., Guggenberger, G., Gatzek, C., Kalbitz, K., 2011. A new conceptual
- model for the fate of lignin in decomposing plant litter. Ecology 92, 1052-1062.
- Kolton, M., Rolando, J.L., Kostka, J.E., 2020. Elucidation of the rhizosphere microbiome linked
- 758 to Spartina alterniflora phenotype in a salt marsh on Skidaway Island, Georgia, USA. FEMS
- 759 Microbiology Ecology 96.
- Komada, T., Polly, J.A., Johnson, L., 2012. Transformations of carbon in anoxic marine
- sediments: Implications from Δ^{14} C and δ^{13} C signatures. Limnology and Oceanography 57, 567-
- 762 581.

- Koop-Jakobsen, K., Mueller, P., Meier, R.J., Liebsch, G., Jensen, K., 2018. Plant-Sediment
- Interactions in Salt Marshes An Optode Imaging Study of O2, pH, and CO2 Gradients in the
- 765 Rhizosphere. Frontiers in Plant Science 9.
- Koretsky, C.M., Haveman, M., Cuellar, A., Beuving, L., Shattuck, T., Wagner, M., 2008.
- Influence of Spartina and Juneus on Saltmarsh Sediments. I. Pore Water Geochemistry.
- 768 Chemical Geology 255, 87-99.
- Koretsky, C.M., Moore, C.M., Lowe, K.L., Meile, C., DiChristina, T.J., Van Cappellen, P., 2003.
- 770 Seasonal oscillation of microbial iron and sulfate reduction in saltmarsh sediments (Sapelo
- Island, GA, USA). Biogeochemistry 64, 179-203.
- Kostka, J.E., Gribsholt, B., Petrie, E., Dalton, D., Skelton, H., Kristensen, E., 2002a. The rates
- and pathways of carbon oxidation in bioturbated saltmarsh sediments. Limnology and
- 774 Oceanography 47, 230-240.
- Kostka, J.E., Roychoudhury, A., Van Cappellen, P., 2002b. Rates and controls of anaerobic
- microbial respiration across spatial and temporal gradients in saltmarsh sediments.
- Biogeochemistry 60, 49-76.
- Kraffczyk, I., Trolldenier, G., Beringer, H., 1984. Soluble root exudates of maize: Influence of
- potassium supply and rhizosphere microorganisms. Soil Biology and Biochemistry 16, 315-322.
- 780 Kristensen, E., Ahmed, S.I., Devol, A.H., 1995. Aerobic and anaerobic decomposition of organic
- matter in marine sediment: Which is fastest? Limnology and Oceanography 40, 1430-1437.
- 782 Kristensen, E., Holmer, M., 2001. Decomposition of plant materials in marine sediment exposed
- to different electron acceptors (O2, NO3-, and SO42-), with emphasis on substrate origin,
- degradation kinetics, and the role of bioturbation. Geochimica et Cosmochimica Acta 65, 419-
- 785 433.

- LaCroix, R.E., Tfaily, M.M., McCreight, M., Jones, M.E., Spokas, L., Keiluweit, M., 2019.
- 787 Shifting mineral and redox controls on carbon cycling in seasonally flooded mineral soils.
- 788 Biogeosciences 16, 2573-2589.
- Lefcheck, J.S., 2016. piecewiseSEM: Piecewise structural equation modelling in r for ecology,
- evolution, and systematics. Methods in Ecology and Evolution 7, 573-579.
- Lin, C.Y., Turchyn, A.V., Krylov, A., Antler, G., 2020. The microbially driven formation of
- respectively. siderite in salt marsh sediments. Geobiology 18, 207-224.
- Lin, Y., Campbell, A.N., Bhattacharyya, A., DiDonato, N., Thompson, A.M., Tfaily, M.M.,
- Nico, P.S., Silver, W.L., Pett-Ridge, J., 2021. Differential effects of redox conditions on the
- decomposition of litter and soil organic matter. Biogeochemistry 154, 1-15.
- Luk, S.Y., Todd-Brown, K., Eagle, M., McNichol, A.P., Sanderman, J., Gosselin, K., Spivak,
- A.C., 2021. Soil Organic Carbon Development and Turnover in Natural and Disturbed Salt
- Marsh Environments. Geophysical Research Letters 48, e2020GL090287.
- 799 Luther, G.W., Findlay, A., MacDonald, D., Owings, S., Hanson, T., Beinart, R., Girguis, P.,
- 2011. Thermodynamics and Kinetics of Sulfide Oxidation by Oxygen: A Look at Inorganically
- 801 Controlled Reactions and Biologically Mediated Processes in the Environment. Frontiers in
- 802 Microbiology 2.
- Luther, G.W., Giblin, A., Howarth, R.W., Ryans, R.A., 1982. Pyrite and oxidized iron mineral
- phases formed from pyrite oxidation in salt marsh and estuarine sediments. Geochimica et
- 805 Cosmochimica Acta 46, 2665-2669.
- Luther, G.W., Kostka, J.E., Church, T.M., Sulzberger, B., Stumm, W., 1992. Seasonal iron
- 807 cycling in the salt-marsh sedimentary environment: the importance of ligand complexes with

- Fe(II) and Fe(III) in the dissolution of Fe(III) minerals and pyrite, respectively. Marine
- 809 Chemistry 40, 81-103.
- Malik, A.A., Martiny, J.B.H., Brodie, E.L., Martiny, A.C., Treseder, K.K., Allison, S.D., 2020.
- Defining trait-based microbial strategies with consequences for soil carbon cycling under climate
- change. The Isme Journal 14, 1-9.
- Mau, R.L., Liu, C.M., Aziz, M., Schwartz, E., Dijkstra, P., Marks, J.C., Price, L.B., Keim, P.,
- Hungate, B.A., 2015. Linking soil bacterial biodiversity and soil carbon stability. The Isme
- 815 Journal 9, 1477-1480.
- Megonigal, J.P., Hines, M.E., Visscher, P., 2003. Anaerobic metabolism: linkages to trace gases
- and aerobic processes, In: Holland, H., Turekian, K.K. (Eds.), Treatise on geochemistry.
- 818 Pergamon, Oxford, pp. 317-424.
- Megonigal, J.P., Whalen, S.C., Tissue, D.T., Bovard, B.D., Allen, A.S., Albert, D.B., 1999. A
- plant-soil-atmosphere microcosm for tracing radiocarbon from photosynthesis through
- methanogenesis. Soil Sci. Soc. Am. J. 63, 665-671.
- Mortimer, R.J.G., Galsworthy, A.M.J., Bottrell, S.H., Wilmot, L.E., Newton, R.J., 2011.
- 823 Experimental evidence for rapid biotic and abiotic reduction of Fe (III) at low temperatures in
- salt marsh sediments: a possible mechanism for formation of modern sedimentary siderite
- concretions. Sedimentology 58, 1514-1529.
- Mozdzer, T.J., Meschter, J., Baldwin, A.H., Caplan, J.S., Megonigal, J.P., 2023. Mining of Deep
- Nitrogen Facilitates Phragmites australis Invasion in Coastal Saltmarshes. Estuaries and Coasts
- 828 46, 998-1008.
- Mueller, P., Jensen, K., Megonigal, J.P., 2016. Plants mediate soil organic matter decomposition
- in response to sea level rise. Global Change Biology 22, 404-414.

- 831 Muyzer, G., Stams, A.J.M., 2008. The ecology and biotechnology of sulphate-reducing bacteria.
- Nature Reviews Microbiology 6, 441-454.
- Noyce, G.L., Megonigal, J.P., 2021. Biogeochemical and plant trait mechanisms drive enhanced
- methane emissions in response to whole-ecosystem warming. Biogeosciences 18, 2449-2463.
- Noyce, G.L., Smith, A.J., Kirwan, M.L., Rich, R.L., Megonigal, J.P., 2023. Oxygen priming
- induced by elevated CO2 reduces carbon accumulation and methane emissions in coastal
- wetlands. Nature Geoscience 16, 63-68.
- Pallud, C., Meile, C., Laverman, A.M., Abell, J., Van Cappellen, P., 2007. The use of flow-
- through sediment reactors in biogeochemical kinetics: Methodology and examples of
- applications. Marine Chemistry 106, 256-271.
- Pett-Ridge, J., Shi, S., Estera-Molina, K., Nuccio, E., Yuan, M., Rijkers, R., Swenson, T.,
- Zhalnina, K., Northen, T., Zhou, J., Firestone, M.K., 2021. Rhizosphere Carbon Turnover from
- Cradle to Grave: The Role of Microbe–Plant Interactions, In: Gupta, V.V.S.R., Sharma, A.K.
- (Eds.), Rhizosphere Biology: Interactions Between Microbes and Plants. Springer Singapore,
- 845 Singapore, pp. 51-73.
- Pinheiro, J., Bates, D., DebRoy, S., Sarkar, D., Team, R.C., 2016. nlme: Linear and nonlinear
- mixed effects models, 3.1-128 ed. R package.
- R Development Core Team, 2022. R: A language and environment for statistical computing. R
- 849 Foundation for Statistical Computing, Vienna.
- Rolando, J.L., Kolton, M., Song, T., Kostka, J.E., 2022. The core root microbiome of Spartina
- alterniflora is predominated by sulfur-oxidizing and sulfate-reducing bacteria in Georgia salt
- marshes, USA. Microbiome 10, 37.

- Roychoudhury, A.N., Van Cappellen, P., Kostka, J.E., Viollier, E., 2003. Kinetics of microbially
- mediated reactions: dissimilatory sulfate reduction in saltmarsh sediments (Sapelo Island,
- Georgia, USA). Estuarine, Coastal and Shelf Science 56, 1001-1010.
- 856 Saintilan, N., Kovalenko, K.E., Guntenspergen, G., Rogers, K., Lynch, J.C., Cahoon, D.R.,
- Lovelock, C.E., Friess, D.A., Ashe, E., Krauss, K.W., Cormier, N., Spencer, T., Adams, J., Raw,
- J., Ibanez, C., Scarton, F., Temmerman, S., Meire, P., Maris, T., Thorne, K., Brazner, J.,
- 859 Chmura, G.L., Bowron, T., Gamage, V.P., Cressman, K., Endris, C., Marconi, C., Marcum, P.,
- St. Laurent, K., Reay, W., Raposa, K.B., Garwood, J.A., Khan, N., 2022. Constraints on the
- adjustment of tidal marshes to accelerating sea level rise. Science 377, 523-527.
- Schippers, A., Jørgensen, B.B., 2002. Biogeochemistry of pyrite and iron sulfide oxidation in
- marine sediments. Geochimica et Cosmochimica Acta 66, 85-92.
- Silveira, M.L., Comerford, N.B., Reddy, K.R., Cooper, W.T., El-Rifai, H., 2008.
- 865 Characterization of soil organic carbon pools by acid hydrolysis. Geoderma 144, 405-414.
- Simpson, A.J., Simpson, M.J., Smith, E., Kelleher, B.P., 2007. Microbially Derived Inputs to
- 867 Soil Organic Matter: Are Current Estimates Too Low? Environmental Science & Technology 41,
- 868 8070-8076.
- 869 Spivak, A.C., 2015. Benthic biogeochemical responses to changing estuary trophic state and
- 870 nutrient availability: A paired field and mesocosm experiment approach. Limnology and
- 871 Oceanography 60, 3-21.
- 872 Spivak, A.C., Denmark, A., Gosselin, K.M., Sylva, S.P., 2020. Salt Marsh Pond
- 873 Biogeochemistry Changes Hourly-to-Yearly but Does Not Scale With Dimensions or Geospatial
- Position. Journal of Geophysical Research: Biogeosciences 125, e2020JG005664.

- 875 Spivak, A.C., Gosselin, K.M., Sylva, S.P., 2018. Shallow ponds are biogeochemically distinct
- habitats in salt marsh ecosystems. Limnology and Oceanography 63, 1622-1642.
- 877 Spivak, A.C., Reeve, J., 2015. Rapid cycling of recently fixed carbon in a Spartina alterniflora
- system: A stable isotope tracer experiment. Biogeochemistry 125, 97-114.
- 879 Spivak, A.C., Sanderman, J., Bowen, J.L., Canuel, E.A., Hopkinson, C.S., 2019. Global-change
- controls on soil-carbon accumulation and loss in coastal vegetated ecosystems. Nature
- 881 Geoscience 12, 685-692.
- 882 Sun, M.-Y.i., Aller, R.C., Lee, C., Wakeham, S.G., 2002. Effects of oxygen and redox oscillation
- on degradation of cell-associated lipids in surficial marine sediments. Geochimica et
- 884 Cosmochimica Acta 66, 2003-2012.
- 885 Sundby, B., Vale, C., Caetano, M., Luther, G.W., 2003. Redox Chemistry in the Root Zone of a
- 886 Salt Marsh Sediment in the Tagus Estuary, Portugal. Aquatic Geochemistry 9, 257-271.
- Sutton-Grier, A.E., Megonigal, J.P., 2011. Plant species traits regulate methane production in
- freshwater wetland soils. Soil Biology and Biochemistry 43, 413-420.
- Thomas, F., Giblin, A.E., Cardon, Z.G., Sievert, S.M., 2014. Rhizosphere heterogeneity shapes
- abundance and activity of sulfur-oxidizing bacteria in vegetated salt marsh sediments. Frontiers
- in Microbiology 5.
- Törnqvist, T.E., Cahoon, D.R., Morris, J.T., Day, J.W., 2021. Coastal Wetland Resilience,
- Accelerated Sea-Level Rise, and the Importance of Timescale. AGU Advances 2,
- e2020AV000334.
- Walter, L.M., Ku, T.C.W., Muehlenbachs, K., Patterson, W.P., Bonnell, L., 2007. Controls on
- the δ^{13} C of dissolved inorganic carbon in marine pore waters: An integrated case study of isotope
- 897 exchange during syndepositional recrystallization of biogenic carbonate sediments (South

- 898 Florida Platform, USA). Deep Sea Research Part II: Topical Studies in Oceanography 54, 1163-
- 899 1200.
- Wang, S.R., Di Iorio, D., Cai, W.-J., Hopkinson, C.S., 2018. Inorganic carbon and oxygen
- 901 dynamics in a marsh-dominated estuary. Limnology and Oceanography 63, 47-71.
- Wang, Y.P., Jiang, J., Chen-Charpentier, B., Agusto, F.B., Hastings, A., Hoffman, F.,
- Rasmussen, M., Smith, M.J., Todd-Brown, K., Wang, Y., Xu, X., Luo, Y.Q., 2016. Responses of
- two nonlinear microbial models to warming and increased carbon input. Biogeosciences 13, 887-
- 905 902.
- 906 Weston, N.B., Dixon, R.E., Joye, S.B., 2006a. Ramifications of increased salinity in tidal
- 907 freshwater sediments: Geochemistry and microbial pathways of organic matter mineralization.
- Journal of Geophysical Research: Biogeosciences 111, G01009.
- 909 Weston, N.B., Porubsky, W.P., Samarkin, V.A., Erickson, M., Macavoy, S.E., Joye, S.B., 2006b.
- Porewater Stoichiometry of Terminal Metabolic Products, Sulfate, and Dissolved Organic
- 911 Carbon and Nitrogen in Estuarine Intertidal Creek-bank Sediments. Biogeochemistry 77, 375-
- 912 408.
- 913 Wieder, W.R., Bonan, G.B., Allison, S.D., 2013. Global soil carbon projections are improved by
- 914 modelling microbial processes. Nature Climate Change 3, 909-912.
- 915 Wirsen, C.O., Sievert, S.M., Cavanaugh, C.M., Molyneaux, S.J., Ahmad, A., Taylor, L.T.,
- DeLong, E.F., Taylor, C.D., 2002. Characterization of an Autotrophic Sulfide-Oxidizing Marine
- 917 <i>Arcobacter</i> sp. That Produces Filamentous Sulfur. Applied and Environmental
- 918 Microbiology 68, 316-325.

Wolfe, A.A., Drake, B.G., Erickson, J.E., Megonigal, J.P., 2007. An oxygen-mediated positive
feedback between elevated carbon dioxide and soil organic matter decomposition in a simulated
anaerobic wetland. Global Change Biology 13, 2036-2044.
Zhang, H., Li, Y., Pang, M., Xi, M., Kong, F., 2019. Responses of Contents and Structure of
DOM to Spartina alterniflora Invasion in Yanghe Estuary Wetland of Jiaozhou Bay, China.
Wetlands 39, 729-741.